Overview of Planar Magnetic Technology—Fundamental Properties

Ziwei Ouyang, *Member, IEEE*, and Michael A. E. Andersen, *Member, IEEE*

***Abstract*—The momentum toward high efficiency, high frequency, and high power density in power supplies limits wide use of conventional wire-wound magnetic components. This paper gives an overview of planar magnetic technologies with respect to the development of modern power electronics. The major advantages and disadvantages in the use of planar magnetics for high-frequency power converters are covered, and publications on planar magnetics are reviewed. A detailed survey of winding conduction loss, leakage inductance, and winding capacitance for planar magnetics is presented so power electronics engineers and researchers can have a clear understanding of the intrinsic properties of planar magnetics.**

***Index Terms*—Fringing effect, inductor, leakage inductance and winding capacitance, parallel winding, planar magnetics, planar sandwiched magnetics, transformer, winding loss.**

I. Introduction

TODAY, high efficiency and high power density converters are fundamental to the continued profitable growth of the telecommunications, automotive, aerospace, and data processing industries. High-frequency operation can lead to a reduction in magnetics size and an increase in power density. The momentum toward high efficiency, high frequency, and high power density in power supplies limits wide use of conventional wire-wound magnetic component structures. For instance, winding loss is significantly increased due to the eddy current effect in conventional round conductors particularly at frequencies above 100 kHz. Moreover, wire-wound magnetic components have resisted the trend toward integration and planarization. Planar magnetic components intrinsically provide lower profiles than conventional wire-wound components, aiding the miniaturization of power converters. Research on the fabrication of planar magnetic components has been investigated since the 1960s [1]. Earlier research into planar magnetics has focused mainly on thin-film technology, specifically for IC design [1]–[3]. Much research related to the design, modeling, and optimization of planar magnetic components emerged in the early 1990s [4]–[6]. In recent years, with the rapid development of printed circuit board (PCB) technology, research into miniature power converters with low-profile cores and PCB winding technologies has attracted widespread international attention [7]–[18].

Manuscript received February 19, 2013; revised May 9, 2013, July 10, 2013, July 22, 2013, and August 13, 2013; accepted September 9, 2013. Date of current version April 30, 2014. Recommended for publication by Associate Editor C. R. Sullivan.

The authors are with the DTU Elektro, Department of Electrical Engineering, Technical University of Denmark, Lyngby 2800, Denmark (e-mail: zo@elektro.dtu.dk; ma@elektro.dtu.dk).

Color versions of one or more of the figures in this paper are available online at http://ieeexplore.ieee.org.

Digital Object Identifier 10.1109/TPEL.2013.2283263

As we have seen the widespread use of planar magnetics in both industry and the academy in recent years, we found it valuable to write an overview of planar magnetic technologies, allowing for researchers and power electronics engineers have more insight into the intrinsic properties of planar magnetics. A small number of studies [19]–[21] have presented surveys of planar magnetic technology. However, the most recent survey [21] was published 12 years ago. With the improvement of PCB technology and the efforts put into planar magnetics over the past 12 years, it is necessary to update the technical overview. This paper gives a detailed overview of planar magnetics in terms of their fundamental properties, including winding loss, leakage inductance, and winding capacitance. Integrated magnetics with planar cores and PCB technology have proven to be effective means of reducing dc–dc converter size, weight and cost, and increasing converter efficiency. Planar magnetic integration technology is not covered in this paper.

II. Characteristics of Planar Magnetic Components

Planar-wound structures are generally created by laminating planar copper windings and disk-like dielectrics into multilayer PCBs that are enclosed by a low-profile magnetically permeable core. The planar cores offer high effective areas for the given effective volumes, efficiently using the magnetic material. It must be noted that the rise in effective area for a given volume is achieved by shrinking the height of the winding window; thus, the window area is reduced. However, the window area is often not fully utilized in a high-frequency design; therefore, shrinking the window area is possible with practically no penalty. The major advantages for the use of planar magnetics are summarized as follows:

1) *Low profile*—planar magnetic components essentially provide lower profiles than conventional wire-wound components, aiding miniaturization. Generally, the height of a planar magnetic component is 1/4 to 1/2 the height of its wire-wound counterpart.
2) *Good thermal characteristic and high power density*—planar magnetic cores essentially have a higher surface area to volume ratio than conventional magnetic cores. As a result, they are more efficient to conduct heat and lead to low temperature rises compared with conventional wire-wound components. Fig. 1 shows a thermal comparison between a conventional core and a planar core. The two cores feature the same volumes, the cross sections, and the window areas. In addition, the same sizes of aluminum plates are used. A power loss of 2 W is assumed to dissipate in each core. The simulations are operated under the

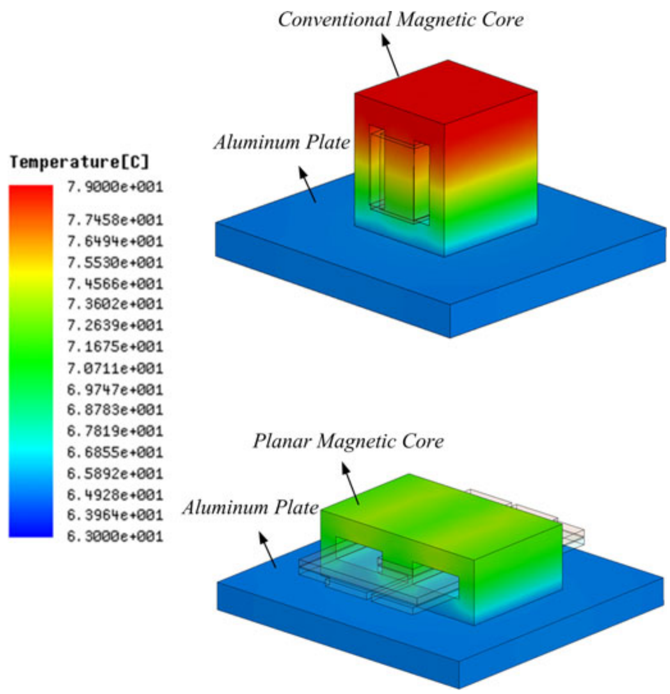

Fig. 1. Comparison of thermal behavior between conventional core and planar core.

same conditions, namely, an ambient temperature of 30 °C and natural heat convection and radiation. It is clear that the planar core provides better thermal behavior than the conventional core. These heat removal benefits add greatly to the power densities, particularly at frequencies ranging from 100 kHz to several MHz. However, it must be noted that this may not be a really fair comparison because the conventional magnetics are generally not connected to a heat exchange surface. Here, the aim is to highlight the advantage of surface-to-volume ratio of planar cores which can provide a better thermal characteristic under the heat exchange surface.

3) *Ease of manufacturability and cost reduction*—the fabrication processes used in planar magnetics relies on advanced computer aided techniques. So it is quite easy to automate the winding of the planar inductors and transformers. PCB techniques are easily adapted for mass production.
4) *Unrivalled repeatability*—the simple automatic assembly process allows planar magnetic components to be fabricated with a high repeatability and accuracy.
5) *Modularity*—because a PCB winding is used for planar magnetic devices, semiconductors and other passive components can also be assembled onto the PCB surfaces. Thus, no extra connections are required.
6) *Ease of implementation on winding interleaving*—as multilayer PCBs allow for an interconnection between arbitrary layers, windings interleaving can be easily implemented. This provides a significant reduction in leakage inductance and high-frequency winding losses.
7) *Predictable parasitics*—it is very difficult to control the winding layout in wire-wound magnetic components. As a result, significant variations in parasitic parameters may appear in devices manufactured at the same time. For planar magnetics, the windings manufactured by PCB machines are more precise and consistent, resulting in magnetic designs with highly controllable and predictable parasitic parameters [22].

The characteristics of planar magnetics are not all advantageous. Some of the limitations are summarized as follows:

1) *Large footprint*—the large surface area offered by the flatter cores is used in planar devices. For simple E-type planar cores, if the core window width is fully utilized, nearly one-third of the PCB winding area will be exposed to the ambient air because the PCB windings are situated in the horizontal direction; this feature will cause a portion of the large footprint. For certain other alternatives, such as ER type cores, the PCB windings can be hidden inside the core; thus, it can have a smaller footprint, but at the expense of reduced core cross section.
2) *Low copper fill factor*—there are safety standards that dictate the minimum distance between windings, influencing the copper fill factor. A typical dielectric material for PCB fabrication is FR4, a composite material composed of woven fiberglass bond with an epoxy resin. The FR4 material standards show an electric strength (breakdown voltage) of approximately 40 kV/mm. Thus, for offline power converters, a minimum distance of 0.1 mm between primary and secondary windings is required to meet safety standards. Besides the consideration of safety standards, a limited PCB fabrication capability also yields a low copper fill factor. If a rigid PCB is used to implement planar windings, a minimum inner-turn spacing of 100 μm and a dielectric thickness of 150 μm are generally required due to the capabilities of PCB fabrication. However, with rapid development of PCB manufacturing and dielectric materials, this limitation can be ameliorated. Copper on a thin flexible polymer substrate (2 MV/mm dielectric strength) gives an improved fill factor, because the dielectric thickness can be made as low as 13 μm. Several single-layer flexible polymer substrates can be laminated together as multiple-layer flexible print circuit board, which results in a similar buildup to a rigid PCB but with higher fill factor.
3) *Limited number of turns*—a low copper fill factor gives a limited number of turns for PCB winding. Furthermore, an increased number of turns require a large number of layers unless the winding width is reduced at the expense of a high dc resistance. Multilayer lamination is not a cost-effective way of implementing the PCB winding because the cost of PCB manufacturing rises rapidly with an increasing number of layers.
4) *High winding capacitance*—stacking windings closely provides an increased winding capacitance, and PCB windings have intrinsically larger surface areas than conventional wire-windings, further increasing the winding capacitance.

In addition to the aforementioned advantages of PCB winding, PCB itself not only performs its initial purpose of electrical interconnection, but also it allows passive components integration of electromagnetic functionality by implementing enhanced substrate materials [23]. This capability allows for packaging 3-D power converters with flexible PCB [11]. Improvement in thermal conduction is achieved by incorporating integration technologies into flexible PCB [24]. Flexible PCBs can improve the copper fill factor in the planar magnetic components due to a thinner polymer substrate. Moreover, incorporating the "z-folding" technique [25] into flexible conductors allows a large number of layers without the need for vias or soldering for layer interconnections. Stamped copper turns provide a cost-effective way of implementing high-current, thick, and single-turn windings. However, additional insulation layers and terminations for layer interconnections are required.

The magnetic material is critical for magnetic component design because core loss is directly determined by the core material. Iron-, cobalt-, and nickel-based metallic alloys, such as FeSi, FeNi, and CoFe are mainly found in low-frequency chokes, current transformers, and current sensors because they usually show high saturation flux densities and some have extremely high permeabilities ($\mu_r > 10\,000$) at low frequencies. Amorphous alloys usually achieve very high permeability with comparable saturation flux density levels. Nanocrystalline materials contain ultrathin crystals that are iron based, giving the material high permeability, high flux density, and good temperature stability. These materials like amorphous and nanocrystalline are often used in medium frequency (up to approximately 100 kHz) invertors, common-mode EMI filters, adjustable speed drives, and power supplies. MnZn Ferrites, such as 3F3 and N87, provide a wide range of permeabilities with relatively low saturation flux densities. Their low electrical conductivities lead to low eddy current losses, making MnZn ferrites suited for high-frequency applications within the range of 100 kHz to 1 MHz. NiZn Ferrites, such as 4F1 and K10, are nearly nonconductivity materials and thus making NiZn ferrites highly suited for the applications within the range of 1 to 100 MHz. However, ferrite is very brittle, and it is difficult to realize an ultrathin sheet. Generally, the thickness of a rigid ferrite plate is more than 1 mm. To avoid breaking, a highly flexible and shock-resistant soft magnetic sheet material FPC (ferrite polymer composites, consisting of ferrite powder in a polymer matrix) was developed. The relative permeability of the FPC material is typically low and ranges from 10 to 20. This low permeability may be sufficient for the design within the megahertz region and may also be used to shielding unwanted magnetic fields in the winding area such as the fringing flux from gapped inductors. Other materials with different composites have been developed to increase the relative permeability and the resistivity, such as IRJ08 from TDK, which consists of ferrite powder and resin. An overview of thin-film magnetic materials for very high frequency (VHF) applications will not be presented in this study. However, [26] and [27] are highly recommended for the relevant contents.

III. Fundamental Properties

A. Winding Loss

The use of a higher switching frequency results in a size reduction in the passive components. This relation is true until a certain frequency limit, where the excessive losses begin increasing the size and the volume of the component [28] and [29]. As with conventional magnetic structures, the demand of high-frequency operation also causes increased winding losses in planar magnetic structures due to skin and proximity effects. Generally, an old-fashioned wire-wound transformer has a high resistance due to the small diameter windings used to overcome the high-frequency eddy current effects (the diameter is selected around skin depth). Thus, it is not allowed to operate at higher power levels unless paralleled wires or litz wires are used. However, planar PCB windings or copper foil have higher width-to-thickness ratios, providing lower dc resistances. In term of winding loss, planar magnetics are more suitable for high-frequency and high-power converters than old-fashioned wire-wound magnetics.

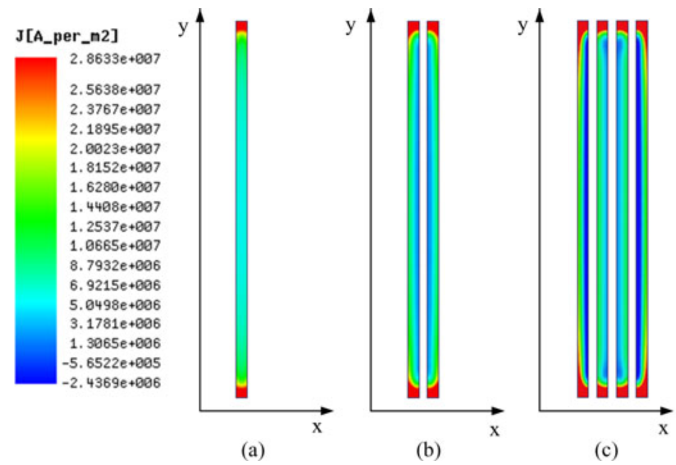

Fig. 2. Current density distribution in a single conductor and multiple conductors without enclosed magnetic cores. (a) Single conductor. (b) Two conductors. (c) Four conductors.

1) Transformer Winding Loss: Winding losses are dramatically increased at high frequency due to eddy current effects. To design an optimal transformer, there is a need for accurate prediction of the winding losses over a wide frequency range and a variety of winding arrangements. Eddy current losses, including skin effects and proximity-effect losses, seriously impair the performance of transformers in high-frequency power conversion applications. For ac current flowing in a conductor, the alternating field inside this conductor induces eddy currents within the conductor, producing a field that tends to cancel that produced by the original current. Therefore, the induced eddy current tends to distribute itself near the surface of the conductor. As a result, the current density near the surface of the conductor is higher than that at its center. This is referred to as the skin effect, causing the effective resistance of the conductor to increase with the frequency of the ac current. The proximity effect is similar, but it is caused by the current carried by an adjacent conductor. This current causes a time-varying field and induces a circulating current inside the conductor. Both the skin effect and the proximity effect cause the current density to be nonuniform in the cross section of the conductor; thus, they cause a high winding resistance at high frequency. Fig. 2 shows current density distribution, based on finite element analysis (FEA), for either a single conductor or multiple conductors without enclosed magnetic cores. The FEA simulation is carried out in the Cartesian *XY* plane with the eddy current solution, and each conductor is excited with the same sinusoidal currents. For a single conductor, the current flow is concentrated at the two ends of conductor because of the skin effect. For multiple conductors, the currents of the conductors tend toward the surface, along the y-axis. This phenomenon is due to the proximity effect caused by adjacent conductors, effectively enhancing the skin effect in each individual conductor. It should be noted that different current distributions occur in practical inductors and transformers with enclosed magnetic cores. This effect is due to the changes in the magnetic field surrounded by the winding turns.

Many efforts have been made to derive expressions that allow for accurate representations of the frequency behavior of an ac resistance. The ac resistance effects due to high-frequency currents are specifically tailored for transformers, as in Dowell [30]. This paper is based on a 1-D solution of the diffusion equation, as applied to conducting parallel plates. Dowell's calculation on transformers is based on the "winding portions" which is defined as a part of a transformer winding containing one position of zero magnetomotive force (MMF) diagram. The MMF at any point across the winding space depends on the total current between the point and the adjacent position of zero MMF. However, this particular approach is subject to some restrictions: 1) the magnetic flux in the winding window (leakage flux) are assumed to be parallel to the surfaces of the conductor layers: if the distances between consecutive turns, between adjacent layers and between the conductor edge, and the magnetic core are small, the induced magnetic field equivalently approaches that of the assumption; 2) the results cannot be applied to the gapped inductor design, in which the energy storage is included, because magnetic field surrounded the air gap (fringing flux) is not parallel to the surfaces of the conductor layers; 3) the excitation voltage and current are sinusoidal; 4) a partial layer, which has substantially less space than the winding window breadth, is not included; 5) infinitely long solenoid windings are assumed. If the windings fill the winding window length completely, the induced magnetic field equivalently approaches that of the assumption; 6) the curvature of the conductors is neglected. Dowell's results in 1966 have been the main references for transformer conduction-loss calculations over the past 50 years. Although their accuracy cannot be guaranteed in practical planar transformer design due to certain restrictions, the most commonly used equation for the winding-loss calculation is still based on Dowell's contribution. Perry analyzed a general N-layer solenoid and derived the winding loss expressions for each rectangle foil layer in 1979 [31]. Venkatraman applied Dowell's results to nonsinusoidal excitation using Fourier analysis in 1984 [32]. Vandelac and Ziogas's work incorporated results of Dowell and Venkatraman to extend Perry's analysis in 1987 [33]. Ferreira rewrote Perry's equation in 1994 and proposed that the orthogonality between the skin effect and proximity effect results in a more generalized approach for the analytical solution of the ac resistance in transformer windings [34]. In 2000, Hurley presented a new formula for the optimum foil or layer thickness, without the need for Fourier coefficients and calculations at harmonic frequencies with arbitrary current waveforms [35]. All of these efforts are based on 1-D calculation methods. A squared-field-derivative method proposed by Sullivan allows for the calculation of losses in multiwinding transformers with 2-D and 3-D field effects and arbitrary waveforms in each winding [36].

Planar winding structures feature flat rectangle copper conductors with higher width-to-thickness ratios. The most commonly used expression for the ac resistance of the mth layer is derived as follows [34]:

$$\frac{R_{\mathrm{ac},m}}{R_{\mathrm{dc},m}} = \frac{\varepsilon}{2}\left[\frac{\sinh\varepsilon+\sin\varepsilon}{\cosh\varepsilon-\cos\varepsilon}+(2m-1)^2\,\frac{\sinh\varepsilon-\sin\varepsilon}{\cosh\varepsilon+\cos\varepsilon}\right] \tag{1}$$

where ε is an effective thickness of the skin depth, which is defined as h/δ, h is the thickness of conductor, and δ is the skin depth at a given frequency. The variable m represents a winding portion and defined as a ratio:

$$m = \frac{F(h)}{F(h)-F(0)} \tag{2}$$

where $F(0)$ and $F(h)$ are the MMFs at the limits of a layer surface. The first term in (1) describes the skin effect factor, and the second term represents the proximity effect factor. The proximity effect loss in a multilayer winding may strongly dominate the skin effect loss, depending on the value of m, which relates to the winding arrangements. The relationship between the eddy current effect, the winding portion m, and the effective thickness of skin depth ε are depicted in Fig. 3. For a large m, the proximity effect dominates over the skin effect, leading to a higher winding resistance. Thinner copper at a given frequency leads to a lower eddy current effect but increases the dc resistance. The optimum thickness of a copper winding can be determined in Fig. 3. Notice that only the sinusoidal current excitation is considered in Fig. 3, and a straightforward expression for the effective ac resistance of a winding with an arbitrary current waveform is suggested in [35]. It may be calculated without knowing the Fourier coefficients of the waveform. The ease of implementation of an interleaved winding is a well-known advantage for planar magnetics. The interleaved winding technique significantly reduces the proximity loss if the currents in the primary and secondary windings are in phase. This effect is due to the reduction in the winding portion m. A fully interleaving structure enables the value of m equal to 1 in each layer. An improved interleaved winding arrangement with the top layer in parallel with the bottom layer, in series with the other turns of the primary, as proposed in [37]; this construction causes the value of m to equal 0.5, further decreasing the winding ac resistance and the leakage inductance. Although (1) can provide relatively good results in a certain frequency range, accurate results are still limited by the aforementioned Dowell's restrictions, particularly for sinusoidal excitations. Moreover, vias are necessary in PCB windings for the multilayer connections, but they will cause additional ac resistances at high frequency. Considering these limitations, accurate winding loss calculation may be determined with the assistance of with 2-D or 3-D FEA tools.

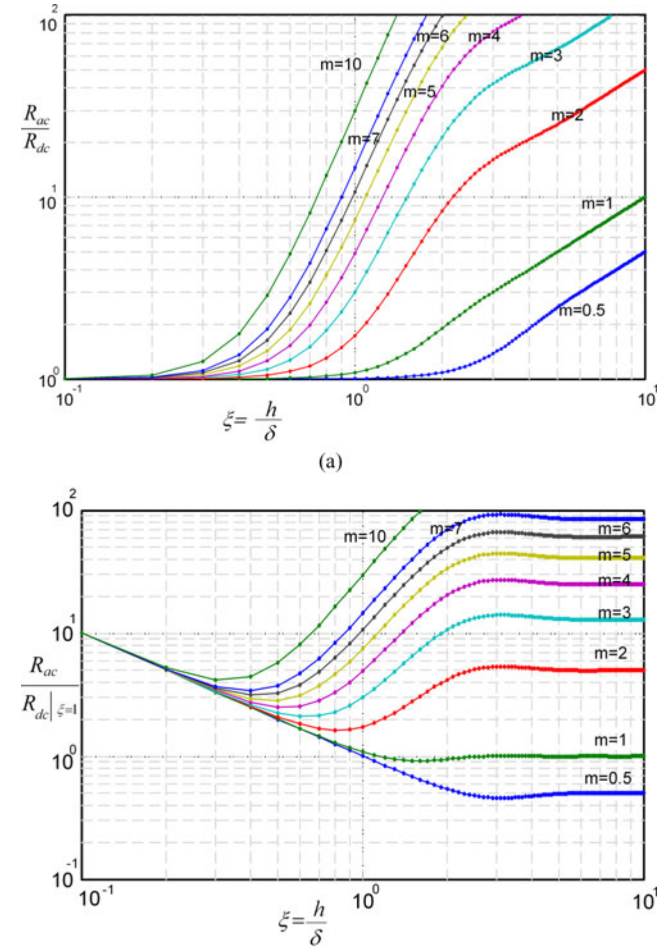

(a)

(b)

Fig. 3. (a) Ratio of the ac resistance to the dc resistance as a function of ε and m; (b) The ac resistance relative to the dc resistance in a layer having an effective thickness of the skin depth.

2) Gapped-Inductor Winding Loss: Due to Dowell's restriction, the 1-D based (1) is not valid for 2-D calculations, such as those for gapped inductors. This limitation is because the external flux through the conductors must be considered. This external flux is caused by the fringing field of air gaps, which further increases the eddy current effect inside the conductors. Hence, in addition to the skin effect loss and proximity effect loss, an excessive power loss caused by the fringing field must be considered for gapped inductors. For those transformers without air gaps, it is relatively straightforward to compute the magnetic field and the resultant losses. However, for gapped inductors, the magnetic field distribution is affected by the gap geometry, the gap position, and the position of conductors. Many efforts have addressed the problem of fringing field losses at high frequencies for planar magnetics [38]–[44]. One excellent set of studies, [43] and [44], shows a calculation methodology for the fringing field for planar inductors. The fringing field is divided into the x component H_x and the y component H_y. For the planar windings situated in the horizontal direction, the x component is parallel to the wide surface of the conductors, and the y component is perpendicular. Both the x and y components

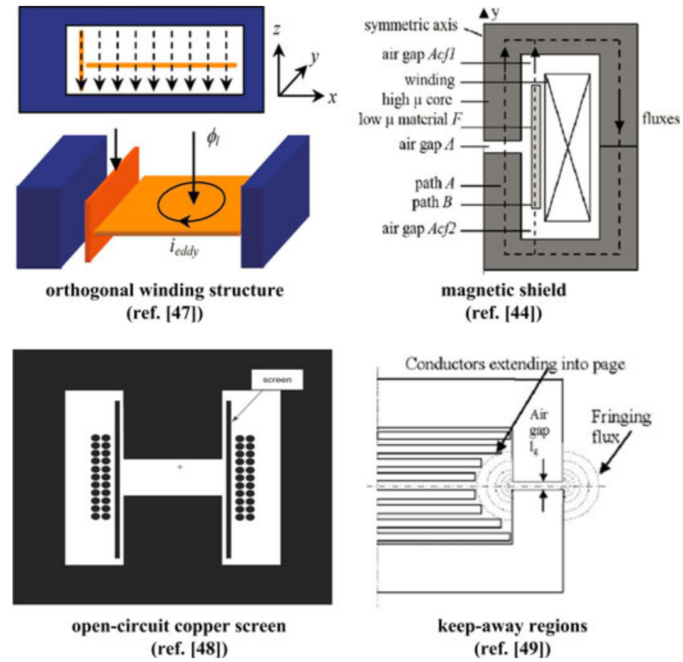

Fig. 4. Typical solutions to minimize the fringing effect.

induce currents flowing toward the edges of the conductor to exclude the external flux. The fringing field loss caused by the x component is small because the thickness of conductor is close to the skin depth. However, the fringing field loss caused by the y component is much higher due to a high width-to-thickness ratio. As shown in Fig. 4, general solutions to minimize the fringing effect are summarized as follows: an orthogonal winding structure is used in [45] to reduce the fringing field loss caused by the y component; a magnetic shield is placed around air gap of a ferrite core to reduce the fringing effect; however, the magnetic shield creates additional flux paths and reduces the total magnetic reluctance, increasing the total inductance [42]; the open-circuit copper screen functions as a flux barrier and reduces the fringing effect because the eddy currents in the copper screen produce a flux that opposes the fringing flux [46]; the copper windings are shaped to create "keep-away regions" to minimize the fringing loss [47]. Moreover, [48] illustrates that the conductors situated far away from the air gaps can also significantly reduce the fringing flux effect.

This paper compares the fringing flux effects for different formats of air gaps. Fig. 5 depicts the current distributions and flux distributions for the gapped inductors based on FEA simulations at 100 kHz; here, the fringing flux effect is illustrated. The same inductances are required for a fair comparison, and the distance between the winding and the air gap is kept the same in all cases. Table I gives a description of six typical gapped inductors and illustrates the fringing effect on winding loss and external magnetic field. For all cases, windings with four turns are arranged at the center of the core window. The current density distribution J has been plotted in the conductors along with the fringing magnetic field H around the air gaps. For cases 1, 2, 4, and 5, the currents must flow toward the ends of conductors to exclude the tangential fringing magnetic field. For cases 3 and 6,

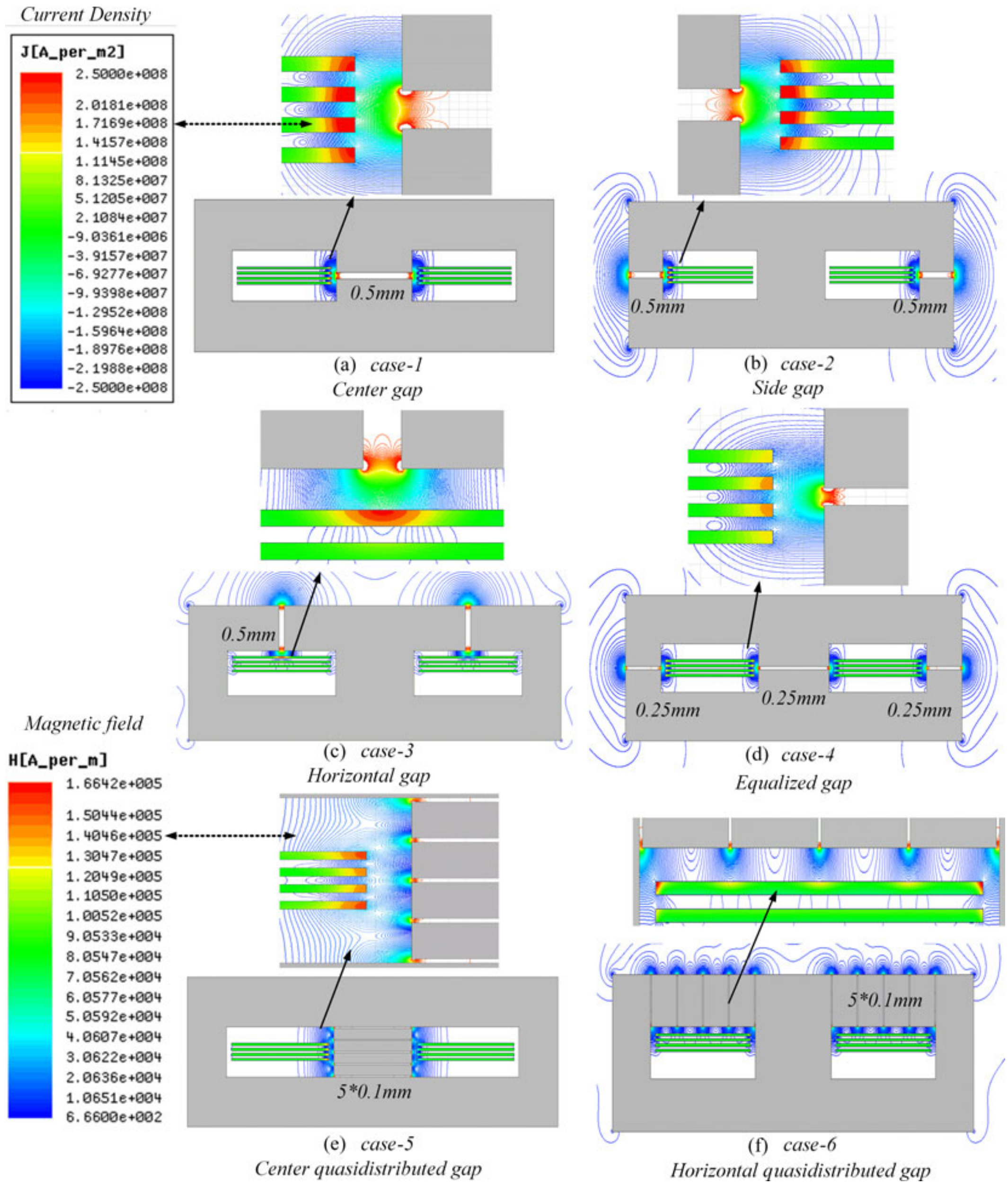

Fig. 5. Current distribution and fringing flux distribution in different formats of air gaps.

the currents flow toward the surfaces of conductors because the tangential fringing magnetic field is parallel to the surfaces of conductors. Because the planar conductors have higher width-to-thickness ratios, the currents crowded at the ends must cause much higher ac resistances than the cases in which the currents crowd at the surfaces.

Fig. 6 shows a comparison of the ratio of the ac resistance to the dc resistance. The center gap (case 1) is the worst case for high-frequency winding loss, in which the ac resistance is 62.8 times the dc resistance at 500 kHz. The center gap generates the most fringing flux perpendicular to the end of conductors, forcing large currents to crowd at the end to exclude the tangential fringing magnetic field. Therefore, the center gap causes the highest ac resistance. The side gap (case 2) has nearly the same fringing effect on the winding resistance as the case of center gap, with a slight reduction at a high frequency. Horizontally arranged gaps give an improved result on ac resistance for planar windings. The ac resistance is 52.2 times the dc resistance at 500 kHz in the horizontal gap (case 3). The equalized gap (case 4) and the center quasidistributed gap (case 5) cases yield significant reductions of the ac resistances because lower fringing magnetic fields are produced by shrinking gap lengths. The ac resistance is 29.7 times the dc resistance at 500 kHz in the case of center quasidistributed gap. The best results are shown in the horizontal quasi-distributed gap (case 6). The ac resistance is only 20.3 times the dc resistance at 500-kHz frequency in this case. The quasi-distributed gap presents an excellent advantage with regard to fringing effect. This technique was presented over

TABLE I
COMPARISON OF SIX TYPICAL GAPPED INDUCTORS

	Description	Fringing effect on winding loss	Fringing effect on external magnetic field
Case 1: **Center gap**	air gap with 0.5-mm length situated at the middle of the center leg	Highest	Low
Case 2: **Side gap**	two air gaps with 0.5-mm length situated at the middle of the side legs	High	High
Case 3: **Horizontal gap**	two air gaps with 0.5-mm length situated at the middle of top core plate	Medium	High
Case 4: **Equalized gap**	three air gaps with 0.25-mm length situated at the middle of all legs	Low	Medium
Case 5: **Center quasi-distributed gap**	quasi-distributed air gaps with 5 interval 0.1-mm gap length situated at the center leg	Low	Low
Case 6: **Horizontal quasi-distributed gap**	quasi-distributed air gaps with 5 interval 0.1-mm gap length situated at the middle of top core plate	Lowest	Medium

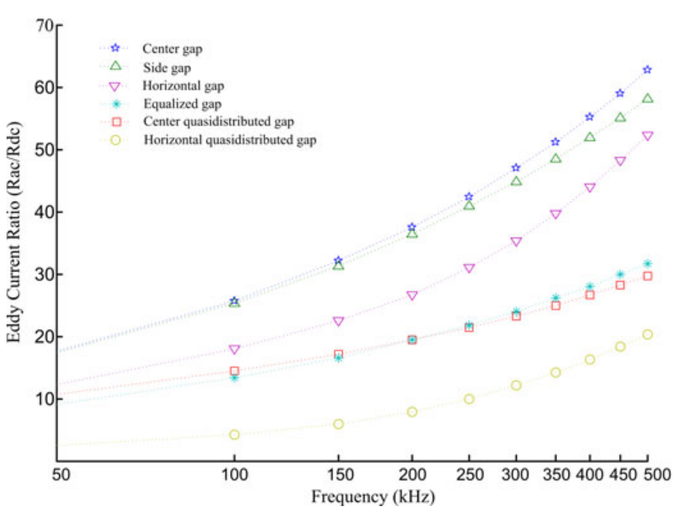

Fig. 6. Comparisons of eddy current effect for different formats of air gaps.

a decade ago [39]. Not only the winding loss needs to be considered for a design of gapped inductors, but the EMI radiation is also an important consideration [49].

3) Winding Loss of Planar Sandwiched Magnetics: The planar magnetic components discussed above are typical planar structures, in which the windings surround the center leg and the core window has a relatively large space. Generally, the flux generated from the windings can be assumed to be uniformly flowing in the core material. As the operational frequency rapidly increases up to the megahertz range, a simple planar design with a sandwiched structure might be a good solution for a low profile requirement. Fig. 7 shows a sandwich transformer structure where the primary and secondary windings patterned on each side of a dielectric layer are sandwiched by two sheets of magnetic material. Generally, this structure and its expansions are applied to PCB embedded power converters [50], [51], thin film technologies [52]–[54], and power supplies on chips [55], [56], all of which have been studied a great deal in recent years. In the planar sandwiched structure, the winding area acts as an air gap; thus, it is a high reluctance path for the magnetic flux. This structure leads to a nonuniform flux distribution, which is not considered in the standard analytical approach. The cases of filament conductors (small width-to-height ratio) in nonconducting magnetic media have been treated in [57] and [58]; these studies have led to inductance models by current images. The formulas presented in these previous studies may not be well suited for wide tracks (high width-to-height ratio) because their nonuniform current densities have not been considered. In [59], a precise impedance formula that includes a nonuniform current distribution and lossy magnetic media was presented. Given that the gap is very thin along the vertical direction, the external flux He in the gap is approximated only in the z-direction, as shown in Fig. 8. The external flux He is tangential to the vertical edges of the conductor, so the current within the conductor has to flow toward the edges in order to exclude the external magnetic field

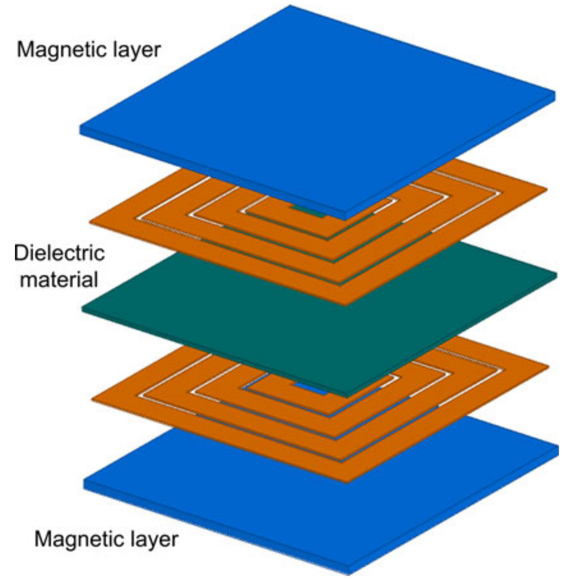

Fig. 7. Planar sandwiched magnetic component.

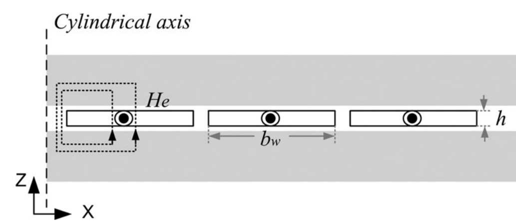

Fig. 8. External flux penetrating to the horizontal surface of conductors.

from the inside of the conductor. The cross-sectional area of the ac current distribution within the conductor is proportional to δ^2 (δ is skin depth), so the effective resistance is much higher than the dc resistance [60]. In [61], the FEA results of eddy current effect at 1 MHz is presented for the planar sandwich coupled inductor. This eddy current effect increases with increased core permeability, in which the ac resistance can reach 65 times than the dc resistance when the relative permeability is 150. The calculation methodology [56] for the winding loss of the sandwiched structure normally uses the orthogonal decomposition of the magnetic field into H_x and H_y, in which the conductors are immersed; this approach is similar to the gapped fringing flux effect.

4) Parallel Windings: Parallel connections of multilayers for planar windings are generally used to increase the current handling capacity. When the windings are in series, the currents in the windings are kept the same, yielding in the same magnetic fields along each layer. When the windings are in parallel, however, the currents in each winding layer may not be equally distributed due to the leakage fluxes and the high-frequency eddy current effect. Thus, the magnetic field around the parallel windings becomes complicated. That is, circulating currents may exist in the parallel layers, causing additional winding loss. Detailed analyses for the parallel effect loss are shown in [62]–[65]. Notice that, with parallel windings, the full interleaved winding arrangement may not be the best case for flyback transformer or the gapped inductor design. This limitation is because the gap fringing effect produces an unbalanced current distribution in the parallel windings [65].

B. Leakage Inductance

Not all the magnetic flux generated by ac current excitation on the primary windings follows the magnetic circuit and links with the secondary windings. The flux linkage between the two windings or parts of the same winding is never complete. A certain degree of flux leaks from the core and returns to the air, winding layers and insulator layers; thus, these flux causes imperfect coupling. The leakage inductance causes the main switch current at the device input to vary at a low slope between zero and the rated value and reduces the rate of commutation between the output diodes. In addition, the stored energy in the leakage inductance leads to a generation of voltage spikes on the main switches, which, aside from creating EMI problems, increases the switching losses and thus reduces the power efficiency [66]. For the normal transformers with low leakage configuration, almost all of the leakage energy is stored within the windings and the space between the windings. The energy associated with the leakage inductance can be calculated according to the analytical MMF distribution and the energy distribution. In Fig. 9, the differential volume of each turn is $l_w \cdot b_w \cdot dx$; therefore, the total energy is the sum of the energy stored in each elementary layer given by the following:

$$E_{\text{energy}} = \frac{\mu_0}{2} \sum \int_0^h H^2 l_w b_w \, dx \quad (3)$$

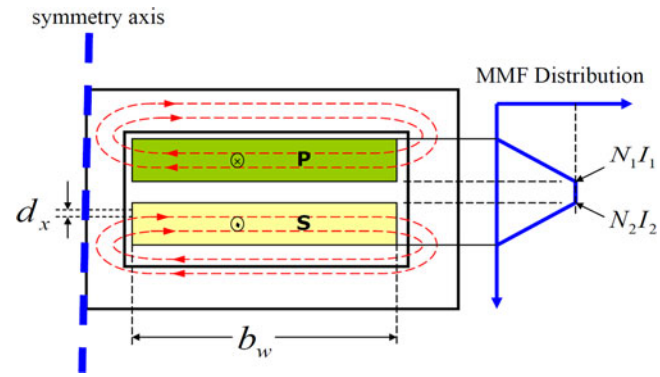

Fig. 9. Leakage flux path and magneto motive force (MMF) variation.

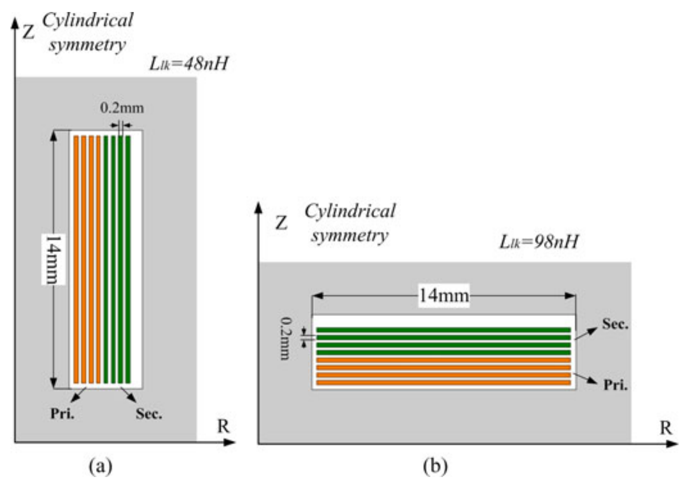

Fig. 10. Comparison of the leakage inductance between a planar structure and a conventional structure. (a) Conventional core geometry with vertical-winding. (b) Planar core geometry with horizontal-winding.

where l_w is the mean turn length (MTL), b_w is the width of each turn, and h represents the thickness of each winding layer. The thickness dx is situated at a distance x from the inner surface of conductor. The field strength H depends on the number of ampere turns linked by the leak flux path. Because the flux return path flows through the high permeability core material, the associated energy is much reduced, and the reluctance of the magnetic path within the magnetic core can be ignored compared with that of the magnetic path in the windings. Thus, the flux path can be expressed by the width b_w rather than the full closed flux path. Therefore, the leakage energy stored within and between the windings is essentially a function of the winding geometry, the core geometry, and the number of turns. An in-depth analysis of the leakage inductance calculation in planar transformer is shown in [67].

Planar transformers have been touted to have low leakage inductances, particularly by certain commercial companies. In fact, planar transformers have been given a misunderstanding that low leakage inductance is an intrinsic property of planar transformers. Fig. 10 shows a comparison of the leakage inductance between a planar structure and a conventional structure. For a fair comparison, the transformer properties, including the cross section and the core volume, the number of turns, the conductor thickness, the space between the conductors and the area of core window were kept the same. According to the FEA simulation, the leakage inductance of a planar structure is twice as large as that of conventional structure. This effect occurs because the planar structure provides a longer MTL, resulting in a higher leakage inductance. More traditional core structures, compared with planar core structures for leakage inductance, are presented in [68]; thus, the planar magnetic has not intrinsically a low leakage inductance. However, the windings may be arranged so as to minimize the leakage inductance. Each coil can be split into sections, and those sections can be placed in layers between the sections of the other winding. This is known as interleaved winding structure. Planar transformers have a significant advantage in this regard because the interleaved winding structure is easily implemented in which a low leakage inductance can be achieved. The interleaved winding reduces the MMF that drives the leakage energy stored. The analysis of leakage inductance reduction by the interleaved winding arrangements and the improved interleaving structure with minimal MMF are presented in [37] and [67]. If the same interleaved winding structure is used in conventional transformer constructions, they will retain their relative leakage inductance advantages over planar transformers. In conclusion, planar transformers do not have the intrinsic property of low leakage inductance. The important benefit of the planar transformer in this regard is relatively easy to interleave the primary and secondary windings.

The methods to reduce the leakage inductance include the following: 1) reduction of the number of turns—based on [67], when neglecting the contribution of fringe fields, the leakage inductance is proportional to the number of turns squared, but the reduction in the number of turns may cause core saturation and higher core loss despite the advantage of the reduced winding conduction loss; 2) reduction of the thicknesses of conductors and insulators—thin copper sheets and insulators can reduce the leakage inductance at the expense of a high dc resistance and high interwinding capacitance; 3) reduction in the mean turn length; 4) increase in the width of conductors; 5) implementation of interleaving winding arrangement.

However, in certain applications, such as a phase-shift-modulated soft-switching dc–dc converter, the magnitude of the leakage inductance determines the achievable load range in zero-voltage-switching operation; thus, a relatively high leakage inductance is required. The aforementioned methods can be used in an opposite way to achieve a desirable high leakage inductance but at the expense of a magnetic field that differs significantly from one parallel to the layers and yielding additional losses. Two additional methods to increase the leakage inductance are described as follows:

1) *Insertion of a magnetic shunt*—between the primary and secondary windings. As shown in Fig. 11, a 0.2 mm ferrite polymer composites (FPC) material with a relative permeability ($\mu_r = 30$) is inserted between the primary and secondary windings, providing a lower reluctance return path for the magnetic flux. This returned magnetic flux does not link to the other windings, in which causes a high leakage and low coupling coefficient. The parameters of core geometry and winding geometry in this transformer are kept the same, as in Fig. 10. The FEA simulation shows that the inserted FPC leads to a four times higher leakage inductance than the case without the FPC. The leakage inductance and the eddy current effect on the windings are respectively plotted as functions of relative permeability of the shunt materials μ_r in Fig. 12. Both leakage inductance and eddy current effect are increased with a higher permeability or a thicker magnetic shunt. Consequently, the magnitude of leakage inductance can be controlled by the thickness and the permeability of the inserted magnetic shunts. The leakage inductance can be calculated by

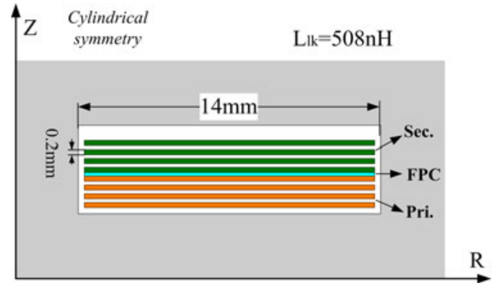

Fig. 11. Leakage inductance with an inserted FPC sheet.

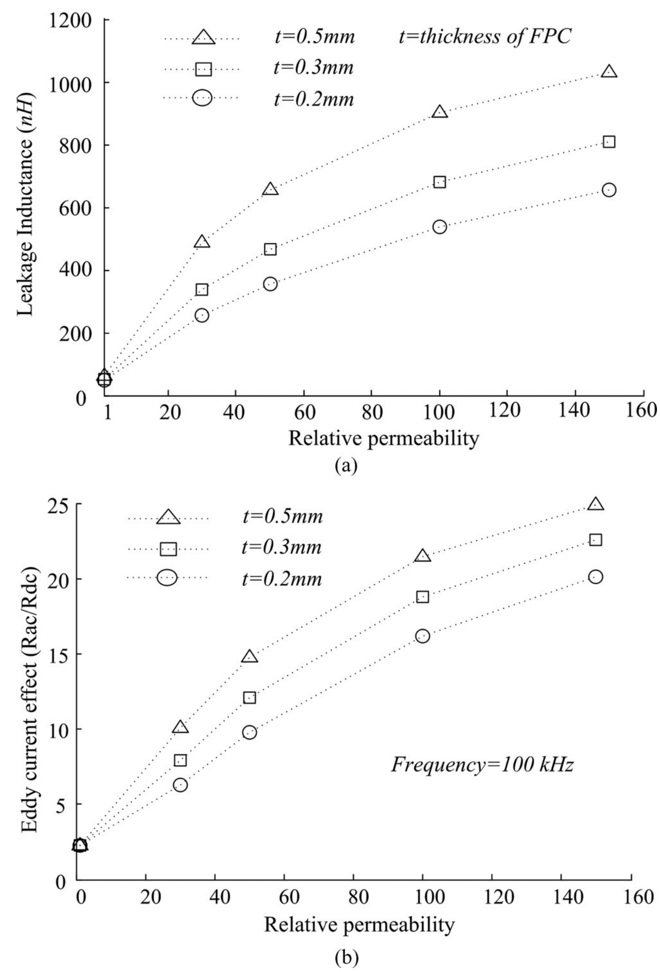

Fig. 12. Functions of leakage inductance (a) and eddy current effect (b) with the relative permeability and the thicknesses of the inserted shunt material.

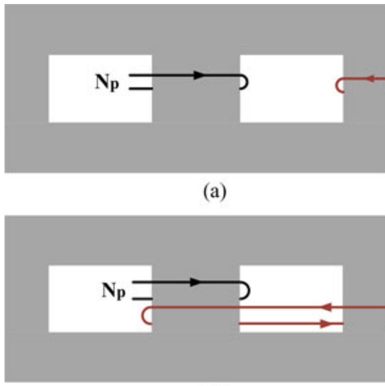

Fig. 13. Examples of fractional turns.

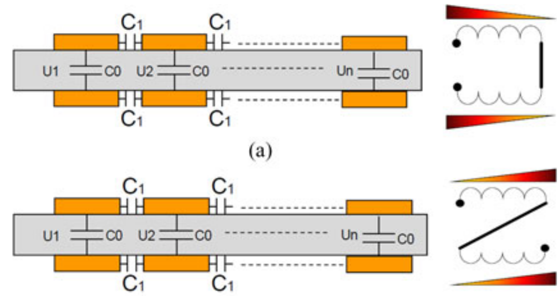

Fig. 14. Voltage distributions along the turns in the adjacent layers: (a) gradual change. (b) constant.

using the methodology of energy storage. The magnetic field stored in the magnetic shunt relies on the ratio of reluctance of the magnetic shunt to that of the main core. A detailed analysis for leakage inductance due to the inserted magnetic shunt is given in [69]. As alternatives to ferrite polymer composites, other magnetic materials such as μ-metal, amorphous iron, or nanocrystalline iron foil can be used to control leakage inductance as well. This approach is often referred to as "integrated magnetics" because a large leakage inductance is formed without adding extra windings, as has been widely used in *LLC* resonant converters [70]–[74].

2) *A fractional turn*—is actually a full turn around a fraction of the total center leg flux. For example, in Fig. 13, each outer leg has half of the total center leg flux as an E–I core shape that has two outer legs of equal cross-sectional areas. A single turn wound around either outer leg will have an induced voltage equal to half of the primary volts per turn. This turn is, therefore, equivalent to a half turn in magnetic reluctance modeling. This type of core splits the magnetic flux into two equal portions, and only one portion is linked with the secondary, resulting in a high leakage inductance. The leakage inductance depends on the ratio of the reluctance of each core leg that the flux is passed by. This approach is not an easy method with which to control the leakage inductance because an uncommon core geometry (custom core design) may be required. The application of fractional turns to an X-type core is presented in [75], and a concrete explanation of the existence of high leakage inductance is given. A similar technique for a high leakage inductance has been applied into a high-power resonant converter [76].

C. Winding Capacitances

There is a tradeoff between leakage inductance and winding capacitances. A lower leakage inductance is achieved at the expense of increased winding capacitances. The winding capacitance cannot be ignored, particularly for planar transformers. The voltage potential between turns, between winding layers, and between windings and core create this parasitic element. Most of the publications for planar transformer design concern the reduction in leakage inductances and high-frequency winding losses, but winding capacitances have rarely been considered effectively. In fact, this parasitic capacitance significantly affects the magnetic component performance, such that the current waveform on the excitation side would be distorted and the overall efficiency of converters would be decreased. Subjected to high-voltage stresses, the interwinding capacitance causes leakage currents and consequently contributes EMI problem [77]–[83]. Methods for examining the parasitic capacitance through the electric field energy distribution along the winding have been addressed in [77], [80], and [82]. The studies in [37] and [79] describe an analytical model for winding capacitances that is valid for planar transformers. The inter- and intrawinding capacitances can be calculated based on the methodology of energy storage, in which a voltage distribution plays a vital role. With a winding connection shown in Fig. 14(b) that provides a constant voltage distribution along the turns in the adjacent layer, the intrawinding capacitance can be significantly reduced compared to the situation that provides different voltage distributions along the turns. Through the analysis of the winding capacitances, the methods for a reduction can be summarized as follows: 1) enhancement of the distance or reduction in the overlapping surface area between the two conductor plates; 2) reduction in the number of turns in each layer and/or increase in the number of layers; 3) reduction in the number of intersections between the primary and the secondary; 4) proper arrangement of the winding connections to obtain the minimal energy associated with the electric field. It is noticed that heavy winding interleaving causes a high capacitance coupling between the primary and secondary windings, which typically increases common-mode noise problems. A grounded electrostatic screen (Faraday shield) is generally inserted between the primary and secondary windings to split and ground the interwinding capacitance, reducing the common-mode noise. The inserted Faraday shield will cause a certain degree of power loss and demagnetization problems (reduction in inductance) due to the eddy current induced in the Faraday shield. A comb-shaped Faraday shield [83] overcomes the aforementioned problems, where the magnetizing inductance is not impacted and the shield power losses can be ignored. However, to date, no method to reduce winding capacitances can reduce leakage inductance. This tradeoff should be taken into account for an optimal design.

For the most transformer designs, the parasitic capacitance is expected to be as small as possible. However, in certain applications in which the circuit is crowded into less space (e.g., integrated *LLC* transformers and EMI filters), the parasitic capacitance is expected to be enhanced, and additional capacitive layers need to be embedded [51], [72], [84]. A dielectric material is sandwiched by two planar layers of conductive windings, thus forming an embedded capacitor. A high or low dielectric permittivity for the dielectric material can be selected as required. The capacitive layers to realize small and medium capacitors are already commercially available. However, high-ε_r capacitive materials for the replacement of electrolytic capacitors are far from being realized. For power electronics purpose, the capacitive layers can be used to replace resonant capacitors, filters, and decoupling and snubber capacitors. The material FR4 is a normal insulator material in the PCB process that exhibits a lower dielectric constant value (DK). This material is comparatively thick and therefore has lower capacitance values. One solution to achieve sufficient capacitance is to add a layer of high DK material between the PCB winding layers. In recent years, there are several companies, such as 3M, Isola, and Rogers, that provide high DK capacitive materials suitable for PCB manufacturing. Another solution is to use a thinner insulator material. To sustain a sufficient breakdown voltage, a polyimide film (Kapton) bonded to copper foil is often required.

IV. Conclusion

This paper gives an overview of planar magnetic technologies with respect to the development of modern power electronics. The major advantages for the use of planar magnetics have been described. A summary of the intrinsic properties of planar magnetics has been given by investigating winding conduction loss, leakage inductance, and winding capacitance. Unlike traditional wire-wound transformers, which use the equivalent porosity factor, planar windings provide straightforward ac resistances under Dowell's contribution. Power electronics engineers must understand the restrictions of Dowell's results so that improved equations might be used to achieve accurate results; these approaches might include a combination with Fourier analysis. Interleaved winding arrangements can significantly reduce the ac resistance. In addition, the fringing effect in the gapped inductor must be taken into account because extremely high eddy current effects are induced in the windings. In recent years, the sandwiched planar structure and its expansions have been widely applied into embedded electronics systems, power supplies on chip and microscaled or nanoscaled integrated systems. The use of this design leads to a nonuniform flux distribution and a good deal of external flux passing through the conductors, causing the standard analytical approach to be invalid for this kind of structure. A visible trend in winding loss considerations for high-frequency magnetic components is the combination of magnetic fields based on 2-D or 3-D FEA simulations with a 1-D analytical approach. A low leakage inductance in the planar transformer has been touted by commercial operations. This study has illustrated that low leakage inductance is not an intrinsic property of the planar transformer, but a higher leakage inductance is provided. The important benefit of the planar transformer in this regard is relatively easy to interleave the primary and secondary windings. The detailed leakage inductance calculations and some suggested methods for reducing leakage inductance are introduced. In certain applications, a high leakage inductance is required, so two additional methods for increasing the leakage are also introduced. High winding capacitance is an intrinsic property of the planar winding transformer and cannot be neglected. The winding capacitance always counteracts the leakage inductance. The voltage potential between turns, between winding layers, and between windings and the core create this parasitic element. Designers must understand that there are many tradeoffs in the use of planar magnetic components. Currently, many publications only address one aspect of magnetic design, potentially yielding excellent solutions for the examined aspect while not considering others. An excellent design must take all aspects and their tradeoffs into account, and the authors expect that power electronics engineers will have excellent ideas in the near future to overcome those tradeoffs without compromising other factors.

References

[1] A. Olivei, "Optimized miniature thin-film planar inductors, compatible with integrated circuits," *IEEE Trans. Parts, Mater. Packag.*, vol. 5, no. 2, pp. 71–88, Jun. 1969.

[2] K. Kawabe, H. Koyama, and K. Shirae, "Planar inductor," *IEEE Trans. Magn.*, vol. 20, no. 5, pp. 1804–1806, Sep. 1984.

[3] O. Oshiro, H. Tsujimoto, and K. Shirae, "A novel miniature planar inductor," *IEEE Trans. Magn.*, vol. 23, no. 5, pp. 3759–3761, Sep. 1987.

[4] L. Heinemann, "Modelling and design of high frequency planar transformers," in *Proc. IEEE Power Electron. Spec. Conf.*, 1995, pp. 651–657.

[5] N. Dai, A. W. Lofti, C. Skutt, W. Tabisz, and F. C. Lee, "A comparative study of high-frequency, low-profile planar transformer technologies," in *Proc. IEEE Appl. Power Electron. Conf. Expo.*, 1994, pp. 226–232.

[6] D. van der Linde, C. A. M. Boon, and J. B. Klaassens, "Design of a high-frequency planar power transformer in multilayer technology," *IEEE Trans. Ind. Electron.*, vol. 38, no. 2, pp. 135–141, Apr. 1991.

[7] R. Prieto, J. A. Cobos, O. Garcia, P. Alou, and J. Uceda, "Using parallel windings in planar magnetic components," in *Proc. IEEE Power Electron. Spec. Conf.*, 2001, pp. 2055–2060.

[8] S. C. Tang, S. Y. R. Hui, and H. S.-H. Chung, "A low-profile power converter using printed-circuit board (PCB) power transformer with ferrite polymer composite," *IEEE Trans. Power Electron.*, vol. 16, no. 4, pp. 493–498, Jul. 2001.

[9] W. Chen, Y.-P. Yan, Y.-Q. Hu, and Q. Lu, "Model and design of PCB parallel winding for planar transformer," *IEEE Trans. Magn.*, vol. 39, no. 5, pp. 3202–3204, Sep. 2003.

[10] L. Dalessandro, N. Karrer, and J. W. Kolar, "High-performance planar isolated current sensor for power electronics applications," *IEEE Trans. Power Electron.*, vol. 22, no. 5, pp. 1682–1692, Sep. 2007.

[11] E. de Jong, J. Ferreira, and P. Bauer, "Toward the next level of PCB usage in power electronic converters," *IEEE Trans. Power Electron.*, vol. 23, no. 6, pp. 3153–3163, Nov. 2008.

[12] C. Buccella, C. Cecati, and F. de Monte, "A coupled electrothermal model for planar transformer temperature distribution computation," *IEEE Trans. Ind. Electron.*, vol. 55, no. 10, pp. 3583–3590, Oct. 2008.

[13] A. Prasai and W. G. Odendaal, "Fabrication and modeling of a planar magnetic structure with directly etched windings," in *Proc. IEEE Energy Convers. Congr. Expo.*, 2009, pp. 1895–1902.

[14] R. Prieto, J. A. Oliver, J. A. Cobos, and M. Christini, "Magnetic component model for planar structures based on transmission lines," *IEEE Trans. Ind. Electron.*, vol. 57, no. 5, pp. 1663–1669, May 2010.

[15] A. W. Roesler, J. M. Schare, S. J. Glass, K. G. Ewsuk, G. Slama, D. Abel, and D. Schofield, "Planar LTCC transformers for high-voltage flyback converters," *IEEE Trans. Compon. Packag. Technol.*, vol. 33, no. 2, pp. 359–372, Jun. 2010.

[16] C. Panchal and J.-W. Lu, "High frequency planar transformer (HFPT) for universal contact-less battery charging platform," *IEEE Trans. Magn.*, vol. 47, no. 10, pp. 2764–2767, Oct. 2011.

[17] S. Djuric, G. Stojanovic, M. Damnjanovic, M. Radovanovic, and E. Laboure, "Design, modeling, and analysis of a compact planar transformer," *IEEE Trans. Magn.*, vol. 48, no. 11, pp. 4135–4138, Nov. 2012.

[18] S. R. Cove, M. Ordonez, F. Luchino, and J. E. Quaicoe, "Applying response surface methodology to small planar transformer winding design," *IEEE Trans. Ind. Electron.*, vol. 60, no. 2, pp. 483–493, Feb. 2013.

[19] M. T. Quirke, J. J. Barrett, and M. Hayes, "Planar magnetic component technology-a review," *IEEE Trans. Compon., Hybrids, Manuf. Technol.*, vol. 15, no. 5, pp. 884–892, Oct. 1992.

[20] J.-P. Schauwers, C. Nunes, B. Velaerts, F. Robert, and P. Mathys, "Planar transformer technology applied to AC/DC conversion," presented at IEEE Telecommun. Energy Conf., Copenhagen, Denmark, 1999.

[21] C. Quinn, K. Rinne, T. O'Donnell, M. Duffy, and C. O. Mathuna, "A review of planar magnetic techniques and technologies," in *Proc. IEEE Appl. Power Electron. Conf. Expo.*, 2001, pp. 1175–1183.

[22] W. G. Hurley and W. H. Wolfle, *Transformers and Inductors for Power Electronics: Theory, Design and Applications*, 1st ed. New York, NY, USA: Wiley, 2013.

[23] E. Waffenschmidt and J. Ferreira, "Embedded passives integrated circuits for power converters," in *Proc. IEEE Power Electron. Spec. Conf.*, 2002, pp. 12–17.

[24] E. de Jong, J. Ferreira, and P. Bauer, "Improving the thermal management of AC-DC converters using integration technologies," in *Proc. IEEE Ind. Appl. Conf.*, 2004, pp. 2315–2322.

[25] K. D. T. Ngo, R. P. Alley, and A. J. Yerman, "Fabrication method for a winding assembly with a large number of planar layers," *IEEE Trans. Power Electron.*, vol. 8, no. 1, pp. 55–61, Jan. 1993.

[26] C. O. Mathúna, N. Wang, S. Kulkarni, and S. Roy, "Review of integrated magnetics for power supply on chip (PwrSoC)," *IEEE Trans. Power Electron.*, vol. 27, no. 11, pp. 4799–4816, Nov. 2012.

[27] C. R. Sullivan, D. V. Harburg, J. Qiu, C. G. Levey, and D. Yao, "Integrating magnetics for on-chip power: A perspective," *IEEE Trans. Power Electron.*, vol. 28, no. 9, pp. 4342–4353, Sep. 2013.

[28] W.-J. Gu and R. Liu, "A study of volume and weight vs. frequency for high-frequency transformers," in *Proc. IEEE Power Electron. Spec. Conf.*, 1993, pp. 1123–1129.

[29] D. J. Perreault, J. Hu, J. M. Rivas, Y. Han, O. Leitermann, R. C. N. Pilawa-Podgurski, A. Sagneri, and C. R. Sullivan, "Opportunities and challenges in very high frequency power conversion," in *Proc. IEEE Appl. Power Electron. Conf. Expo.*, 2009, pp. 1–14.

[30] P. L. Dowell, "Effects of eddy currents in transformer windings," in *Proc. Inst. Elect. Eng.*, Aug. 1966, vol. 113, no. 8, pp. 1387–1394.

[31] M. P. Perry, "Multiple layer series connected winding design for minimum losses," *IEEE Trans. Power App. Syst.*, vol. PAS-98, no. 1, pp. 116–123, Jan. 1979.

[32] P. S. Venkatraman, "Winding eddy current losses in switch mode power transformers due to rectangular wave currents," in *Proc. 11th Power Conversion Conf.*, 1984, sec. A-1, pp. 1–11.

[33] J. P. Vandelac and P. D. Ziogas, "A novel approach for minimizing high frequency transformer copper losses," *IEEE Trans. Power Electron.*, vol. 3, no. 3, pp. 266–277, Jul. 1988.

[34] J. Ferreira, "Improved analytical modeling of conductive losses in magnetic components," *IEEE Trans. Power Electron.*, vol. 9, no. 1, pp. 127–131, Jan. 1994.

[35] W. G. Hurley, E. Gath, and J. G. Breslin, "Optimizing the AC resistance of multilayer transformer windings with arbitrary current waveforms," *IEEE Trans. Power Electron.*, vol. 15, no. 2, pp. 369–376, Mar. 2008.

[36] C. R. Sullivan, "Computationally efficient winding loss calculation with multiple windings, arbitrary waveforms, and two-dimensional or three-dimensional field geometry," *IEEE Trans. Power Electron.*, vol. 16, no. 1, pp. 142–150, Jan. 2001.

[37] Z. Ouyang, O. C. Thomsen, and M. A. E. Andersen, "Optimal design and tradeoff analysis of planar transformer in high power dc–dc converters," *IEEE Trans. Ind. Electron.*, vol. 59, no. 7, pp. 2800–2810, Jul. 2012.

[38] N. H. Kutkut and D. M. Divan, "Optimal air-gap design in high-frequency foil windings," *IEEE Trans. Power Electron.*, vol. 13, no. 5, pp. 942–949, Sep. 1998.

[39] J. Hu and C. R. Sullivan, "AC resistance of planar power inductors and the quasidistributed gap technique," *IEEE Trans. Power Electron.*, vol. 16, no. 4, pp. 558–567, Jul. 2001.

[40] P. Wallmeier, "Improved analytical modeling of conductive losses in gapped high-frequency inductors," *IEEE Trans. Ind. Appl.*, vol. 37, no. 4, pp. 1045–1054, Jul./Aug. 2001.

[41] M. Albach and H. Robmanith, "The influence of air gap size and winding position on the proximity losses in high frequency transformers," in *Proc. IEEE Power Electron. Spec. Conf.*, 2001, pp. 1485–1490.

[42] X. Mao, W. Chen, and Y. Li, "Winding loss mechanism analysis and design for new structure high-frequency gapped inductor," *IEEE Trans. Magn.*, vol. 41, no. 10, pp. 4036–4038, Oct. 2005.

[43] W. A. Roshen, "Fringing field formulas and winding loss due to an air gap," *IEEE Trans. Magn.*, vol. 43, no. 8, pp. 3387–3394, Aug. 2007.

[44] W. A. Roshen, "High-frequency fringing fields loss in thick rectangular and round wire windings," *IEEE Trans. Magn.*, vol. 44, no. 10, pp. 2396–2401, Oct. 2008.

[45] J. Sun and V. Mehrotra, "Orthogonal winding structures and design for planar integrated magnetics," *IEEE Trans. Ind. Electron.*, vol. 55, no. 3, pp. 1463–1469, Mar. 2008.

[46] J. Fletcher, B. Williams, and M. Mahmoud, "Airgap fringing flux reduction in inductors using open-circuit copper screens," in *IEE Proc. Electric Power Appl.*, Jul. 2005, vol. 152, no. 4, pp. 990–996.

[47] L. Ye, G. R. Skutt, R. Wolf, and F. C. Lee, "Improved winding design for planar inductors," in *IEEE Proc. Power Electron. Spec. Conf.*, 1997, pp. 1561–1567.

[48] Z. Ouyang, G. Sen, O. C. Thomsen, and M. A. E. Andersen, "Analysis and design of fully integrated planar magnetics for primary-parallel isolated boost converter," *IEEE Trans. Ind. Electron.*, vol. 60, no. 2, pp. 494–508, Feb. 2013.

[49] K. D. Papastergiou and D. E. Macpherson, "Air-gap effects in inductive energy transfer," in *Proc. IEEE Power Electron. Spec. Conf.*, 2008, pp. 4092–4097.

[50] M. Ludwig, M. Duffy, T. O'Donnell, P. McCloskey, and S. C. Mathuna, "PCB integrated inductors for low power dc-dc converter," *IEEE Trans. Power Electron.*, vol. 18, no. 4, pp. 937–945, Jul. 2003.

[51] E. Waffenschmidt, B. Ackermann, and J. A. Ferreira, "Design method and material technologies for passives in printed circuit board embedded circuits," *IEEE Trans. Power Electron.*, vol. 20, no. 3, pp. 576–584, May 2005.

[52] Y. Fukuda, T. Inoue, T. Mizoguchi, S. Yatabe, and Y. Tachi, "Planar inductor with ferrite layers for DC-DC converter," *IEEE Trans. Magn.*, vol. 39, no. 4, pp. 2057–2061, Jul. 2003.

[53] N. Wang,, T. O'Donnell, R. Meere, F. M. F. Rhen, S. C. Ó. Mathúna, and S. Roy, "Thin film integrated power inductor on Si and its performance in a 8 MHz buck," *IEEE Trans. Magn.*, vol. 44, no. 11, pp. 4096–4099, Nov. 2008.

[54] J. Qiu and C. R. Sullivan, "Design and fabrication of VHF tapped power inductors using nanogranular magnetic films," *IEEE Trans. Power Electron.*, vol. 27, no. 12, pp. 4965–4975, Dec. 2012.

[55] C. O. Mathúna, N. Wang, S. Kulkarni, and S. Roy, "Review of integrated magnetics for power supply on chip (PwrSoC)," *IEEE Trans. Power Electron.*, vol. 27, no. 11, pp. 4799–4816, Nov. 2012.

[56] N. Wang, T. O'Donnell, and C. O'Mathuna, "An improved calculation of copper losses in integrated power inductors on silicon," *IEEE Trans. Power Electron.*, vol. 28, no. 8, pp. 3641–3647, Aug. 2013.

[57] W. A. Roshen, "Effect of finite thickness of magnetic substrate on planar inductors," *IEEE Trans. Mag.*, vol. 26, no. 1, pp. 270–275, Jan. 1990.

[58] W. A. Roshen, "Analysis of planar sandwich inductors by current images," *IEEE Trans. on Mag.*, vol. 26, no. 5, pp. 2880–2887, Sep. 1990.

[59] W. G. Hurley and M. C. Duffy, "Calculation of self- and mutual impedances in planar sandwich inductors," *IEEE Trans. Mag.*, vol. 33, no. 3, pp. 2282–2290, May. 1997.

[60] A. F. Goldberg, J. G. Kassakian, and M. F. Schlecht, "Issues related to 1–10 MHz transformer design," *IEEE Trans. Power Electron.*, vol. 4, no. 1, pp. 113–123, Jan. 1989.

[61] Z. Ouyang, M. Acanski, J. Popovic-Gerber, J. A. Ferreira, O. C. Thomsen, and M. A. E. Andersen, "Design consideration of ultra-thin coupled inductors for photovoltaic application," in *Proc. IEEE Integr. Power Electron. Syst.*, 2012, pp. 1–8.

[62] W. Chen, Y.-P. Yan, Y.-Q. Hu, and Q. Lu, "Model and design of PCB parallel winding for planar transformer," *IEEE Trans. Magn.*, vol. 39, no. 5, pp. 3202–3204, Sep. 2003.

[63] X. Margueron, J.-P. Keradec, and A. Besri, "Current sharing between parallel turns of a planar transformer: Prediction and improvement using a circuit simulation software," in *Proc. IEEE Ind. Appl. Conf.*, 2007, pp. 1787–1793.

[64] R. Prieto, J. A. Cobos, O. Garcia, P. Alou, and J. Uceda, "Using parallel windings in planar magnetic components," in *Proc. IEEE Power Electron. Spec. Conf.*, 2001, pp. 2055–2060.

[65] R. Prieto, R. Asensi, and J. A. Cobos, "Selection of the appropriate winding setup in planar inductors with parallel windings," in *Proc. IEEE Energy Convers. Congr. Expo.*, 2010, pp. 4599–4604.

[66] W. G. Hurley and D. J. Wilcox, "Calculation of leakage inductance in transformer windings," *IEEE Trans. Power Electron.*, vol. 9, no. 1, pp. 121–126, Jan. 1994.

[67] Z. Ouyang, O. C. Thomsen, and M. A. E. Andersen, "The analysis and comparison of leakage inductance in different winding arrangements for planar transformer," in *Proc. IEEE Power Electron. Drive Systems*, Nov. 2009, pp. 1143–1148.

[68] B. W. Carsten, "The low leakage inductance of planar transformers; fact or myth?" in *Proc. IEEE Appl. Power Electron. Conf. Expo.*, 2001, pp. 1184–1188.

[69] J. Zhang, Z. Ouyang, M. C. Duffy, M. A. E. Andersen, and W. G. Hurley, "Leakage inductance calculation for planar transformers with magnetic shunt," in *Proc. IEEE Energy Convers. Congr. Expo.*, 2013, pp. 643–648.

[70] M. Meinhardt, M. Duffy, T. O'Donnell, S. O'Reilly, J. Flannery, and C. O Mathuna, "New method for integration of resonant inductor and transformer-design, realisation, measurements," in *Proc. IEEE Appl. Power Electron. Conf. Expo.*, 1999, pp. 1168–1174.

[71] I. W. Hofsajer, J. A. Ferreira, and J. D. van Wyk, "Design and analysis of planar integrated L-C-T components for converters," *IEEE Trans. Power Electron.*, vol. 15, no. 6, pp. 1221–1227, Nov. 2000.

[72] R. Chen, J. T. Strydom, and J. D. van Wyk, "Design of planar integrated passive module for zero-voltage-switched asymmetrical half-bridgePWM converter," *IEEE Trans. Ind. Appl.*, vol. 39, no. 36, pp. 1648–1655, Nov./Dec. 2003.

[73] W. Liu and J. D. van Wyk, "Design of integrated LLCT module for LLC resonant converter," in *Proc. IEEE Appl. Power Electron. Conf. Expo.*, 2005, pp. 362–368.

[74] Y. Liang, W. Liu, B. Lu, and J. D. van Wyk, "Design of integrated passive component for a 1 MHz 1 kW half-bridge LLC resonant converter," in *Proc. IEEE Ind. Appl. Conf.*, 2005, pp. 2223–2228.

[75] G. Perica, "Elimination of leakage effects related to the use of windings with fractions of turns," *IEEE Trans. Power Electron.*, vol. PE-1, no. 1, pp. 39–47, Jan. 1986.

[76] J. Biela and J. W. Kolar, "Electromagnetic integration of high power resonant circuits comprising high leakage inductance transformers," in *Proc. IEEE Power Electron. Spec. Conf.*, 2004, pp. 4537–4545.

[77] T. Duerbaum and G. Sauerlaender, "Energy based capacitance model for magnetic devices," in *Proc. IEEE Appl. Power Electron. Conf. Expo.*, 2001, pp. 109–115.

[78] H.-Y. Lu, J.-G. Zhu, and S. Y. R. Hui, "Experimental determination of stray capacitances in high frequency transformers," *IEEE Trans. Power Electron.*, vol. 18, no. 5, pp. 1105–1112, Sep. 2003.

[79] B. Ackermann, A. Lewalter, and E. Waffenschmidt, "Analytical modelling of winding capacitances and dielectric losses for planar transformers," in *Proc. IEEE Workshop Comput. Power Electron.*, Aug. 15–18, 2004, pp. 2–9.

[80] L. Dalessandro, F. S. Cavalcante, and J. W. Kolar, "Self-capacitance of high-voltage transformers," *IEEE Trans. Power Electron.*, vol. 22, no. 5, pp. 2081–2092, Sep. 2007.

[81] J. Biela and J. W. Kolar, "Using transformer parasitics for resonant converters—A review of the calculation of the stray capacitance of transformers," *IEEE Trans. Ind. Appl.*, vol. 44, no. 1, pp. 223–233, Jan./Feb. 2008.

[82] C. K. Lee, Y. P. Su, and S. Y. R. Hui, "Printed spiral winding inductor with wide frequency bandwidth," *IEEE Trans. Power Electron.*, vol. 26, no. 10, pp. 2936–2945, Oct. 2011.

[83] J. Lu and F. Dawson, "Characterizations of high frequency planar transformer with a novel comb-shaped shield," *IEEE Trans. Magn.*, vol. 47, no. 10, pp. 4493–4496, Oct. 2011.

[84] R. Chen, J. D. Van Wyk, S. Wang, and W. G. Odendaal, "Improving the characteristics of integrated EMI filters by embedded conductive layers," *IEEE Trans. Power Electron.*, vol. 20, no. 3, pp. 611–619, May 2005.

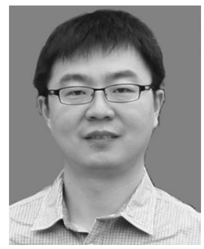

Ziwei Ouyang (S'07–M'11) received the B.S. degree in electrical engineering from the Naval University of Engineering, Wuhan, China, in 2004, the M.S. degree from the Tianjin University of Technology, Tianjin, China, in 2007, and the Ph.D. degree from the Technical University of Denmark (DTU), Kongens Lyngby, Denmark, in 2011.

He has been with the Gelsenkirchen University of Applied Science, Technical University of Delft and National University of Ireland, as a Visiting Scholar, in 2006, 2011, and 2013, respectively. Since 2011, he has been with the Technical University of Denmark as a Postdoctoral Researcher where he is currently Assistant Professor in the Department of Electrical Engineering. His current research interests include advanced magnetics design, modeling, and integration in switch mode power supplies, dc/dc converters, and digital control in high-power reversible converters.

Dr. Ouyang received the Chinese Government Award for Outstanding Ph.D. Students Abroad in 2010 and he received Best Ph.D. dissertation of the Year Award 2012 in Technical University of Denmark. He has more than 30 peer-reviewed journal and conference publications and he is the holder of three U.S./EP/PCT patents with one pending. He received the Best Paper Awards in ECCE-Asia conferences in 2010 and 2012, respectively. He has served as Session Chair in conferences and reviewer for IEEE TRANSACTIONS ON POWER ELECTRONICS and IEEE TRANSACTIONS ON INDUSTRIAL ELECTRONICS. He is member of the PELS, IES, and Magnetics societies.

Michael A. E. Andersen (M'88) received the M.Sc.E.E. and Ph.D. degrees in power electronics from the Technical University of Denmark, Kongens Lyngby, Denmark, in 1987 and 1990, respectively.

He is currently a Professor of power electronics with the Technical University of Denmark, where he is the Deputy Director in the Department of Electrical Engineering as well as the Head of the Danish Ph.D. Research School in Electrical Energy Systems "EnergyLabDK." He has authored or coauthored more than 100 papers. His research interests include switch-mode power supplies, piezoelectric transformers, power factor correction, and switch-mode audio power amplifiers.